15th Triennial World Congress, Barcelona, Spain

LIMITATIONS IN THE CONTROL OF A DC-DC BOOST CONVERTER

Cunha, F. B. [*,1] and **Pagano, D. J.** [*]

[*] *Departamento de Automação e Sistemas, Universidade Federal de Santa Catarina, 88040-900, Florianópolis, SC, Brasil*
e-mail: {daniel, felipe}@das.ufsc.br

Abstract: This paper analyses the control of a DC-DC boost converter using both instantaneous and averaged models. The control objectives are discussed and the main focus is the load disturbance rejection. The transient performance is shown to be limited by saturation constraints on the control variable. In particular, it is shown that the transient behaviour of the output voltage in the presence of load disturbances cannot be minimized beyond a certain limit by the control strategy. Simulation results obtained using two different control laws put in evidence these limitations.

Keywords: nonlinear systems, switching systems, DC-DC boost converters, constraints, saturation, adaptive sliding mode control.

1. INTRODUCTION

The DC-DC boost converter is an electronic system which transfers electric power from a voltage source to an output load. The main task of such a system is to provide a regulated output voltage greater than its input voltage (Kassakian *et al.*, 1991). The boost performs this task by means of switching elements that govern the energy transfer from the input to the output. The circuit operation can be divided into two stages: (i) the energy accumulation in the input inductor, (ii) the energy transfer to the output capacitor. The design of this system comprises, among other things, choosing the best way to perform this energy transfer with minimum losses.

Besides these efficiency issues, the boost output should be robust with respect to load changes and fluctuations of the input voltage source. While the efficiency is basically a *design problem*, the disturbance rejection is traditionally a *control problem*. This stated, the main objective in the boost converter control is, in the presence of such disturbances, to drive the output voltage back to its nominal value with a minimum transient behaviour.

This paper intents to show that the transient behaviour of the output voltage in the presence of load disturbances cannot be minimized beyond a certain limit by the control strategy. This limit arises from the inner structural characteristics of the boost converter and can only be minimized if the desired transient behaviour is taken into account in the design phase of this power electronic device.

The paper is organized as follows. Section 2 briefly describes the two main approaches to model the boost converter; section 3 deals with the problem of rejecting load disturbances considering the constraints imposed to the control by the switching nature of the system. Section 4 presents simulation results to compare the performance of two different controllers, a linear PID and an adaptive fixed-frequency sliding mode controller.

[1] Partially supported by COPENE - Petroquímica do Nordeste S.A., Brasil

2. DC-DC BOOST CONVERTER

The basic circuit topology of the DC-DC boost converter is given in Fig. 1. All components are considered ideal, which means that there is no parasitic resistance associated with the energy storing elements or with the semiconductor elements that perform the switching. The boost can operate in both *continuous conduction mode (CCM)* and *discontinuous conduction mode (DCM)*. The simulation model used in this work incorporates these two possible operation modes of the circuit.

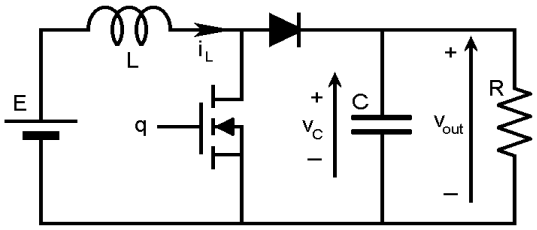

Fig. 1. Ideal DC-DC boost model.

In Fig. 1, R stands for a load resistance and $E > 0$ represents the available voltage source. The voltage v_{out} over R is the system output which should be driven to a regulated desired value $v_{out} = V_C > E$. The inductor current i_L and the capacitor voltage v_C are taken as state variables for a state space representation of the system.

The circuit analysis of the boost converter in Fig. 1 operating in CCM leads to the nonlinear state space equation

$$\begin{cases} \dot{x}_1 = -\dfrac{1}{L}(1-q)x_2 + \dfrac{1}{L}E \\ \dot{x}_2 = \dfrac{1}{C}(1-q)x_1 - \dfrac{1}{RC}x_2 \end{cases} \tag{1}$$

where $x_1 = i_L$, $x_2 = v_C$ and q represents the discrete state of the switch.

It is important to remark that the discontinuous conduction mode can be understood as the result of a constraint in the state variable x_1 expressed by $x_1 \geq 0$. This constraint arises from the diode characteristics. As an indirect consequence, the output voltage represented by x_2 is always non-negative. Note that the instantaneous nonlinear dynamic model expressed by (1) does not take into account these constraints. In order to do so, a more complex hybrid model comprising the continuous and discrete dynamics of the system is necessary.

Eq. (1) is known in the literature as the ideal *instantaneous model*. It describes the instantaneous dynamic of the state variables x_1 and x_2, including the ripple caused by the high frequency switching. This ripple can be eliminated from the model by

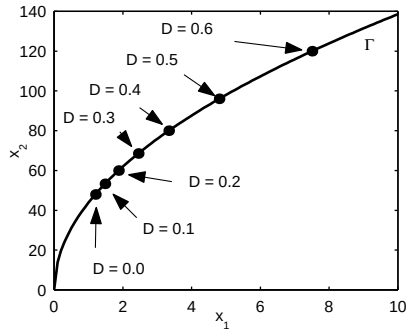

Fig. 2. Equilibrium manifold with d as a parameter.

using the *averaging techniques* described in *Kassakian et al.* (1991) , which leads to an *averaged model* that is formally identical to Eq. (1) with the only difference that the instantaneous discrete variable q is replaced by the continuous duty cycle d and the variables x_1 and x_2 are the time local averages of the instantaneous values of i_L and v_C over one switching period. Each of these two approaches gives rise to different controller families: (i) those based on the instantaneous model and (ii) those based on the averaged model.

No matter how Eq. (1) is treated, the equilibrium points the boost can exhibit are the same. They can be calculated by imposing $\dot{x}_1 = 0$ and $\dot{x}_2 = 0$ and eliminating q from the resulting algebraic system. This procedure gives the following set of possible equilibria:

$$\Gamma = \left\{ (x_1, x_2) \in \mathbf{R}^2 \Big/ x_1 = \frac{{x_2}^2}{RE} \right\} \tag{2}$$

which is a 1-dimension manifold in the state space. All equilibrium points of (1) must lie on the manifold Γ regardless of the function q. When q is replaced by its average d each point in Γ corresponds to the equilibrium associated with a constant value $d = D$. These equilibria are given by (see Fig. 2)

$$\overline{X}_1 = \frac{E}{R(1-D)^2}; \qquad \overline{X}_2 = \frac{E}{(1-D)}. \tag{3}$$

Note that the set Γ depends on the values of R and E.

2.1 *Instantaneous Model*

The controllers designed based on the instantaneous model generally act directly at the switch deciding when it is to be commuted.

To analyse the instantaneous model each operating stage has to be considered separately. When $q = 0$, Eq. (1) becomes

$$\begin{cases} \dot{x}_1 = -\dfrac{1}{L}x_2 + \dfrac{1}{L}E \\ \dot{x}_2 = \dfrac{1}{C}x_1 - \dfrac{1}{RC}x_2. \end{cases} \tag{4}$$

The dynamic system described by Eq. (4) will be referred to as the *0-structure* of the boost converter. This 0-structure exhibits a linear dynamic around the unique equilibrium point

$$\overline{X}_0 = \begin{bmatrix} \bar{x}_{0_1} \\ \bar{x}_{0_2} \end{bmatrix} = \begin{bmatrix} E/R \\ E \end{bmatrix}. \tag{5}$$

The eigenvalues associated with $\overline{X}_0$ are

$$\lambda_{1,2} = -\alpha \pm j\omega = -\tfrac{1}{2RC} \pm j\sqrt{\tfrac{1}{LC} - \left(\tfrac{1}{2RC}\right)^2} \tag{6}$$

assuming that $L < 4R^2C$. A possible pair of eigenvectors is

$$v_1 = \begin{bmatrix} \frac{1}{L} \\ -\lambda_1 \end{bmatrix}, \qquad v_2 = \begin{bmatrix} \frac{1}{L} \\ -\lambda_2 \end{bmatrix}. \tag{7}$$

The analytic solution of this system is

$$\begin{bmatrix} x_1(t) \\ x_2(t) \end{bmatrix} = K_1 v_1 e^{\lambda_1 t} + K_2 v_2 e^{\lambda_2 t} + \overline{X}_0 \tag{8}$$

where K_1 and K_2 are complex conjugate constants chosen to meet the initial conditions $x_1(0) = x_{1_0}$ and $x_2(0) = x_{2_0}$.

When $q = 1$ the system (1) reduces to

$$\begin{cases} \dot{x}_1 = \dfrac{1}{L}E \\ \dot{x}_2 = -\dfrac{1}{RC}x_2. \end{cases} \tag{9}$$

Eq. (9) will be referred to as the *1-structure* of the system (1). This structure has no equilibrium points and its analytic solution is

$$\begin{cases} x_1(t) = x_{1_0} + \frac{E}{L}t \\ x_2(t) = x_{2_0} e^{-\frac{t}{RC}}. \end{cases} \tag{10}$$

All possible trajectories of the system (1), in open or closed loop, are constructed with pieces of the *natural trajectories* given by the solutions (8) and (10). Fig. 3 shows an arbitrary trajectory as an exemple.

2.2 *Averaged and Linearized Models*

Another possible approach to the analysis of the boost converter is to consider Eq. (1) as the averaged model. In this case, the switch is operated by a PWM signal modulated by a continuous control variable d that takes the place of q in (1) and represents its duty cycle.

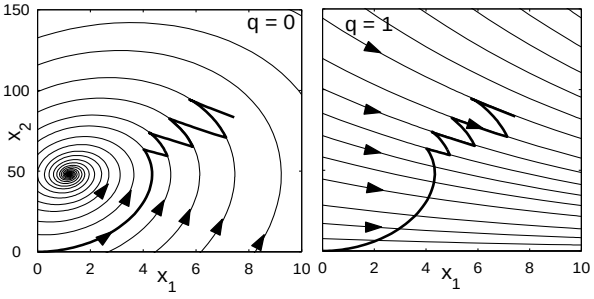

Fig. 3. Natural trajectories.

Continuous nonlinear control functions can be synthesized directly from the averaged nonlinear model (Sira-Ramírez *et al.*, 1997), (Escobar *et al.*, 1999) but the most traditional way to control the boost is to linearize Eq. (1) around the desired equilibrium point and to design a linear controller for the linearized system (Martins *et al.*, 1996). After expanding the righthand side of (1) in Taylor series and neglecting the nonlinear terms, the linearized model becomes

$$\begin{bmatrix} \dot{\tilde{x}}_1 \\ \dot{\tilde{x}}_2 \end{bmatrix} = \begin{bmatrix} 0 & -\frac{(1-D)}{L} \\ \frac{(1-D)}{C} & -\frac{1}{RC} \end{bmatrix} \cdot \begin{bmatrix} \tilde{x}_1 \\ \tilde{x}_2 \end{bmatrix} + \begin{bmatrix} \frac{V_C}{L} \\ -\frac{I_L}{C} \end{bmatrix} \cdot \tilde{d} + \begin{bmatrix} \frac{1}{L} & 0 \\ 0 & \frac{V_C}{R^2C} \end{bmatrix} \cdot \begin{bmatrix} \tilde{e} \\ \tilde{r} \end{bmatrix} \tag{11}$$

where $[I_L\ V_C]^T$ is the desired equilibrium point, D, R and E are the nominal duty cycle, load and voltage source, respectively. The control input is represented by $\tilde{d}$, and the disturbance variables $\tilde{e}$ and $\tilde{r}$ are fluctuations about the nominal values of E and R, respectively. Note that this linearized model is only valid near the operating point and for small load or source disturbances. If the state vector is far from the nominal equilibrium or if the disturbance range is wide, the linearized model loses its validity.

3. CONTROL OBJECTIVES AND CONSTRAINTS

The DC-DC boost converter must be insensitive with respect to load disturbances and fluctuations of the voltage source. Therefore, the main control objectives are to reject these kinds of disturbances with a minimum transient behaviour and to drive the output voltage back to its nominal value. This section focuses on the load disturbance rejection problem from a geometric approach of the saturation constraint on the control variable d.

3.1 *Constraint on the Control*

Under the assumption that the switch operates according to a high frequency PWM control signal,

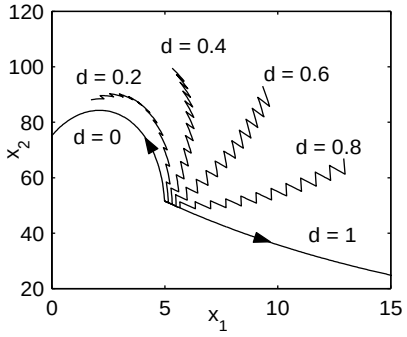

Fig. 4. Range of possible trajectories under constant duty cycle subject to the saturation limits $d = 0$ and $d = 1$.

it is possible to replace the discrete control variable q by its duty cycle d. The control saturation is inherent to this procedure and the saturation limits correspond to the discrete states of the switch. For this reason, the duty cycle can only vary in the real interval [0, 1]. The examples shown in Fig. 4 illustrate this effect. All trajectories start from the same initial condition and evolve according to a fixed duty cycle d. It is clear from Fig. 4 that there is a certain zone below the trajectories with $d = 0$ and $d = 1$ which cannot be achieved directly.

3.2 *Load Disturbance Rejection*

To analyse the load disturbance rejection it is necessary to consider how a change in resistance affects the state space trajectories. The solution for the 1-structure presented in Eq. shows that the current dynamic does not change because $x_1(t)$ does not depend on R. On the other hand, (10) shows that the voltage $x_2(t)$ decays slower with an increase and faster with a decrease in the value of R. The load change in the 0-structure case can be shown to affect the system damping $\xi = \frac{1}{2R}\sqrt{\frac{L}{C}}$ and the value of the equilibrium input current $\bar{x}_{0_1} = \frac{E}{R}$. As stated in section 2, the set Γ, loci of all possible equilibria, also changes under a load disturbance. This effect is shown in Fig. 5.

Suppose that a boost converter is required to operate under a certain load range and that the load increases or decreases instantaneously by step changes. Under these hypotheses, the most critical case occurs when the load changes from its maximum value to its minimum and then returns to its maximum. To illustrate this idea, consider a $250W$ DC-DC boost with $C = 10\mu F$, $L = 1.4mH$, $E = 48V$ and $V_C = 100V$ operating at a $40kHz$ frequency. The load range goes from 20% ($R = 200\Omega$) up to 100% ($R = 40\Omega$) of the nominal power. The equilibrium manifolds corresponding to these two extreme cases are depicted in Fig. 5.

Consider the case where the boost is in steady state working with full load and the output resis-

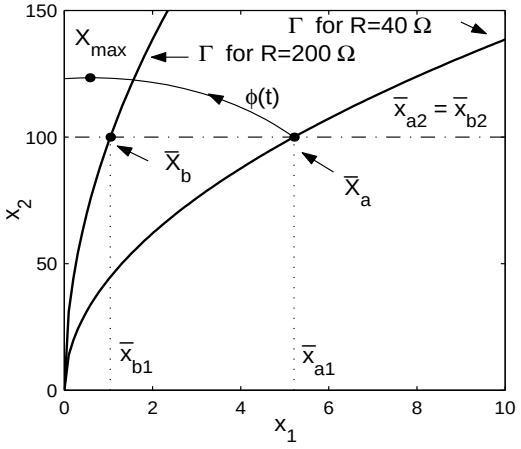

Fig. 5. System trajectory for saturated duty cycle $d = 0$.

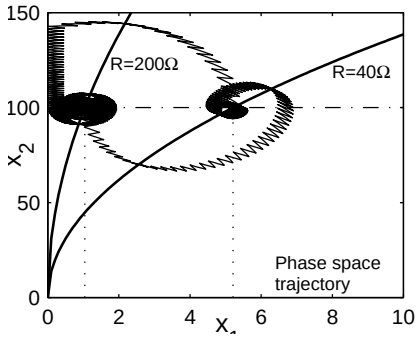

Fig. 6. Phase plane trajectory showing the effect of critical load disturbance.

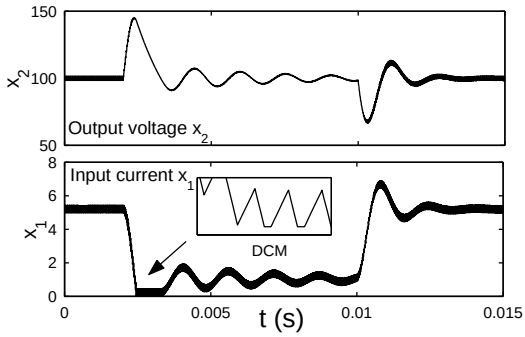

Fig. 7. Effect of load disturbance in the open loop transient behaviour.

tance suddenly changes from $R_a = 40\Omega$ to $R_b = 200\Omega$. The transient behaviour of the open loop boost is poorly damped and exhibits a quite high voltage overshoot (about 45%). Besides, during the transient, the boost operates in *discontinuous conduction mode* for a certain time interval (see Figs. 6 and 7).

Thus, the control task is to drive the system state from $\overline{X}_a$ to $\overline{X}_b$ minimizing this undesirable transient effects. In other words, the current is required to decrease to $\bar{x}_{b_1}$ within minimum time and the voltage must settle in the desired regulated value $\bar{x}_{b_2} = V_C$ after going through a minimum overshoot also within minimum time.

In order to reach the new equilibrium point $\overline{X}_b$ in a short time it is necessary to decrease the inductor current as fast as possible. The only way to do so is to saturate the duty cycle in its minimum value, which means to leave the switch on the position $q = 0$. In this case, the state vector moves along the natural trajectory $\phi(t)$ of the 0-structure of the system (see Fig. 5). This trajectory alone does not lead to the desired equilibrium point. It means that the duty cycle cannot remain in its saturation value. At some point in the $\phi(t)$ trajectory, the controller has to make the decision of changing the value of the duty cycle in order to force the state vector toward the point $\overline{X}_b$. There are basically two options for this decision: (i) to leave the saturation *before* reaching the point X_{max}, or (ii) to leave the saturation *after* reaching X_{max}, which is the point of maximum voltage in the saturated trajectory $\phi(t)$. This point represents the minimum voltage overshoot (about 23%) that can be ideally achieved.

To reduce the voltage overshoot the duty cycle has to increase, leaving the saturated value $d = 0$, before the state vector reaches the maximum point of the natural trajectory. This procedure forces the state vector to move near the equilibrium manifold Γ. In the neighborhood of Γ, the magnitude of the average phase velocity vector is small. This causes the state vector to converge slowly to the new equilibrium point $\overline{X}_b$.

If the state vector is required to converge fast to the equilibrium point, the control has to drive the system through a trajectory far from the equilibrium manifold Γ. If this condition is satisfied, then the state trajectory evolves in a region where the magnitude of the phase velocity vector is higher than when it is near Γ. To reach such a region, the state vector must necessarily pass by the point X_{max}. In this situation, the overshoot cannot be reduced below the point X_{max}. This behaviour becomes clear by analysing the components of the phase velocity vector of each structure of the system.

The above geometric considerations show that the control objectives of minimizing the overshoot and minimizing the settling time are mutually exclusive. Therefore, any compensator designed to control the boost converter cannot achieve both optimum performances. In order to exemplify this limitation, a comparative study of two different controllers is carried out in the next section.

4. COMPARING TWO DIFFERENT CONTROLLERS

Consider first the linearized model (11). The transfer function from the duty cycle to the output voltage is

$$G(s) = -\frac{I_L}{C}\frac{s - \frac{R}{L}(1-D)^2}{s^2 + \frac{1}{RC}s + \frac{(1-D)^2}{LC}} \qquad (12)$$

where $I_L = \frac{V_C^2}{RE}$ and the other parameters are defined in Subsection 3.2.

A linear PID controller was designed by the root-locus method for the linear model. The parameters obtained by this procedure were finely tuned via simulations of the closed loop nonlinear model leading to the following controller:

$$C(s) = 0.3\frac{s^2 + 3000s + 3534^2}{s(s + 2 \times 10^5)}. \qquad (13)$$

A second controller has been designed to be compared with the classic linear PID. An adaptive sliding mode controller that operates in fixed frequency has been developed to achieve load disturbance rejection for the DC-DC boost converter. Unlike traditional sliding mode strategy, a pulse width modulator has been employed to make the interface between the controller and the plant in order to guarantee the fixed frequency operation. The load disturbance rejection is achieved by adaptation of the control parameters via a static estimate of the load resistance R. Its estimate, $\widehat{R}$, is made by calculating the relation between the average output voltage and the average output current. This requires an extra sensor to measure this current. The control law is (DeCarlo *et al.*, 1988)

$$u(x) = u_{eq}(x) + u_N(x) \qquad (14)$$

where

$$\begin{aligned} u_{eq}(x) &= 1 - \frac{s_1 CE - s_2 L\frac{x_2}{\widehat{R}}}{s_1 C x_2 - s_2 L x_1} \\ u_N(x) &= \gamma\sigma(x) = \gamma\left(s_0(\widehat{R}) + s_1 x_1 + s_2 x_2\right). \end{aligned} \qquad (15)$$

In the case of the boost converter, the control variable u is the duty cycle d. The controller parameters are $\gamma = 0.002$, $s_2 = -1$, $s_1 = -55.8$ and $s_0 = -\frac{s_1 {V_C}^2}{E\widehat{R}} - s_2 V_C$.

The phase plane trajectories of the system under these two control laws are depicted in Fig. 8 for a load transition from 40Ω to 200Ω at $t = 2ms$ and back to 40Ω at $t = 10ms$. The time evolution of the state variables and the control input can be seen in Fig. 9 and Fig. 10.

From the results obtained by simulation of the DC-DC boost converter, it can be seen that the qualitative behaviours of the closed-loop boost with the two different controllers are very similar. The settling time for the case of an increase in resistance is about $2ms$ for both controllers. In the case of a decrease in resistance it is approximately

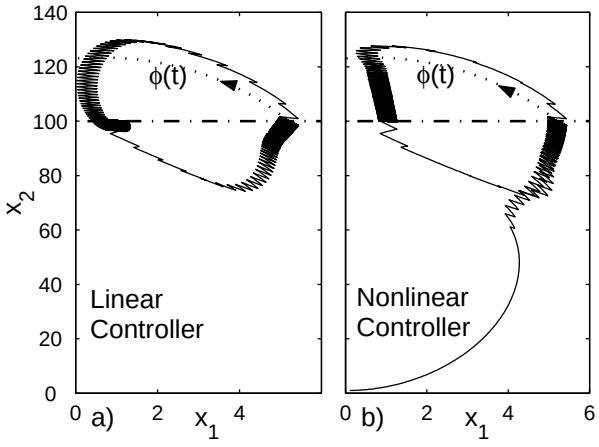

Fig. 8. System trajectories for two different controllers.

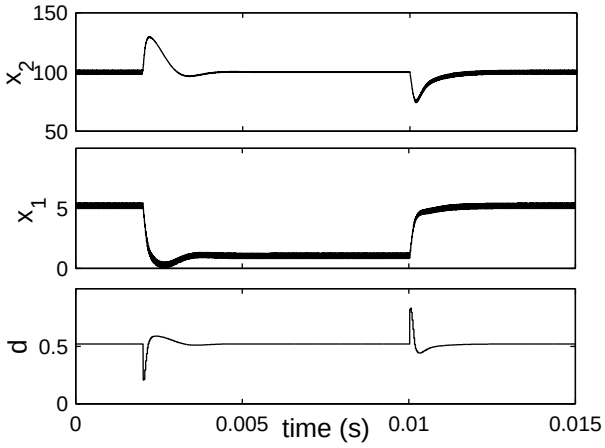

Fig. 9. Time response for the PID controller.

$1ms$. For both controllers the overshoot is about 25% of the nominal output voltage. This similarity is due to the intrinsic constraint on the control variable $0 \leq d \leq 1$. Note that the transient parts of the trajectories in Fig. 8 are very close to the saturated trajectory $\phi(t)$. This indicates that the performance achieved with these two controllers can hardly be further improved, for any better controller would meet the saturation constraint.

Despite the complexity of the nonlinear control, its performance is not expressively better than that of the linear PID controller. Nevertheless, it can be shown that the equilibrium point is globally asymptotically stable when subject to the nonlinear controller. This is not the case for the linear one, for which the equilibrium point is only locally stable and has an attraction basin associated to it. As a consequence of this local stability, when the DC-DC boost converter is controlled using a linear strategy, auxiliary *soft start* circuitry is necessary to drive the system into the region of attraction of the equilibrium point in order for the controller to be able to act.

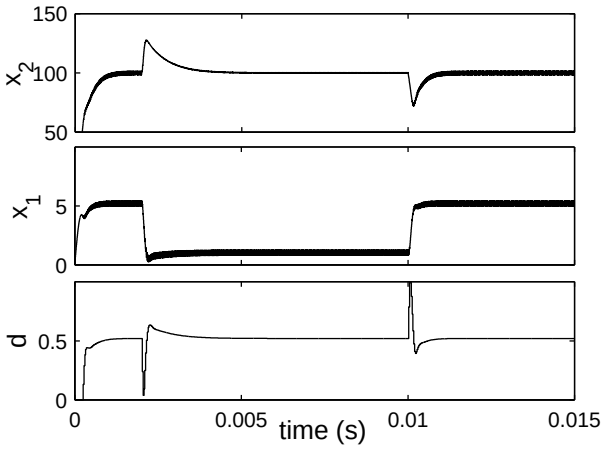

Fig. 10. Time response for the sliding mode controller.

5. CONCLUSIONS

The load disturbance rejection of the DC-DC boost converter was shown to depend on the inner structural characteristics of the system. The saturation of the control variable imposes a definitive limitation on the controller performance. To minimize the effect of load disturbances, the desired transient behaviour of the output voltage has to be considered in the design phase of the system, for any possible controller would be limited by the saturation of the duty cycle.

Since most power electronic devices are based on switching, these kind of saturation effects are always present. This suggests that the results presented in this paper could be extended to other devices.

6. REFERENCES

DeCarlo, R. A., S. H. Zak and G. P. Matthews (1988). Variable structure control of nonlinear multivariable systems: A tutorial. *Proc. of the IEEE,* **76**(3), 212–232.

Escobar, G., R. Ortega, H. Sira-Ramírez, J-P. Vilain and I. Zein (1999). An experimental comparission of several nonlinear controllers for power converters. *IEEE Contr. Sys.,* **19**(1), 66–82.

Kassakian, J. G., M.F. Schlecht and G. C. Verghese (1991). *Principles of Power Electronics.* Addison-Wesley. Massachusetts.

Martins, A. S., E. V. Kassick and I. Barbi (1996). Control strategy for the double-boost converter in continuous conduction mode applied to power factor correction. *PESC* **2**, 1066–1072.

Sira-Ramírez, H., R. A. Perez-Moreno, R. Ortega and M. Garcia-Esteban (1997). Passivity-based controllers for stabilization of dc-to-dc power converters. *Automatica,* **33**(4), 499–513.